Memristive plasticity in artificial electrical synapses via geometrically reconfigurable, gramicidin-doped biomembranes

Subhadeep Koner[1], Joseph S. Najem[2], Md Sakib Hasan[3], Stephen A. Sarles[1]

[1] Department of Mechanical, Aerospace and Biomedical Engineering, University of Tennessee, Knoxville, Tennessee 37916, United States;

[2] Department of Mechanical Engineering, The Pennsylvania State University, University Park, Pennsylvania 16802, United States;

[3] Department of Electrical Engineering, University of Mississippi, Oxford, Mississippi 38677, United States.

*Corresponding author:

Stephen A. Sarles, Department of Mechanical, Aerospace and Biomedical Engineering, University of Tennessee, 308 Dougherty Engineering Bldg., 1512 Middle Dr., Knoxville, TN 37996, Phone: 865-974-3488, email: ssarles@utk.edu

Derivation of state equations for an artificial electrical synapse

The nominal current through our artificial electrical synapse (AES) is given by:

	$I = G(x)V$	S1

where G is the non-linear conductance and x represents multiple, voltage-dependent state variables [1]. The dynamic equations defining the voltage-dependence of the state variables is given by:

	$\frac{dx}{dt} = f(x;V).$	S2

The nonlinear and hysteretic plots of *I-V* in Figures 1 C-E display the voltage-dependent conductance of a memristive AES. Since ions cross the membrane through gramicidin dimers and not via the insulating membrane, the nominal conductance is determined by the total number of gramicidin channels present in the interface. Our experiments further reveal that the number of gramicidin channels per unit area, N_D, and the fractional increase in area, A_m, are the two, independent, voltage-controlled state variables in an AES. Therefore, equation S1 is rewritten as:

	$I = G(N_D,A_m)V$	S3

Voltage dependent dynamic change in membrane area

The area of a droplet interface bilayer (DIB) increases dynamically in response to an increase in net transmembrane voltage due to electrowetting (EW), which reduces the net interfacial tension

of the membrane [2-5]. This relaxation increase changes the contact angle between droplets and, through conservation of droplet volumes, leads to a larger contact (i.e., bilayer) area. The steady state fractional increase in bilayer area at constant thickness, A_m, is given by:

	$$A_m(V) = \frac{A(V) - A_0}{A_0} = \alpha V^2$$	S6

where A_0 and α are the bilayer area at zero volts and voltage sensitivity constant, respectively[4]. Based on observations that changes in area display first-order exponential time responses, we express dynamic fractional changes in area as:

	$$\frac{dA_m}{dt} = \frac{1}{\tau_{ew}}\left(\alpha V^2 - A_m(t)\right)$$	S7

where τ_{ew} is the characteristic time constant for electrowetting.

Nominal conductance, G

With the empirical expressions for voltage-dependent channel density (equations 4 and 5) and the fractional change in area upon electrowetting (equation S7), we write the total conductance term of equation S3 as:

	$$G(V,t) = G_u N_D(V) A_0\left(1 + A_m(V,t)\right)$$	S8

where G_u is the unit conductance single gramicidin channel (5.8 pS).

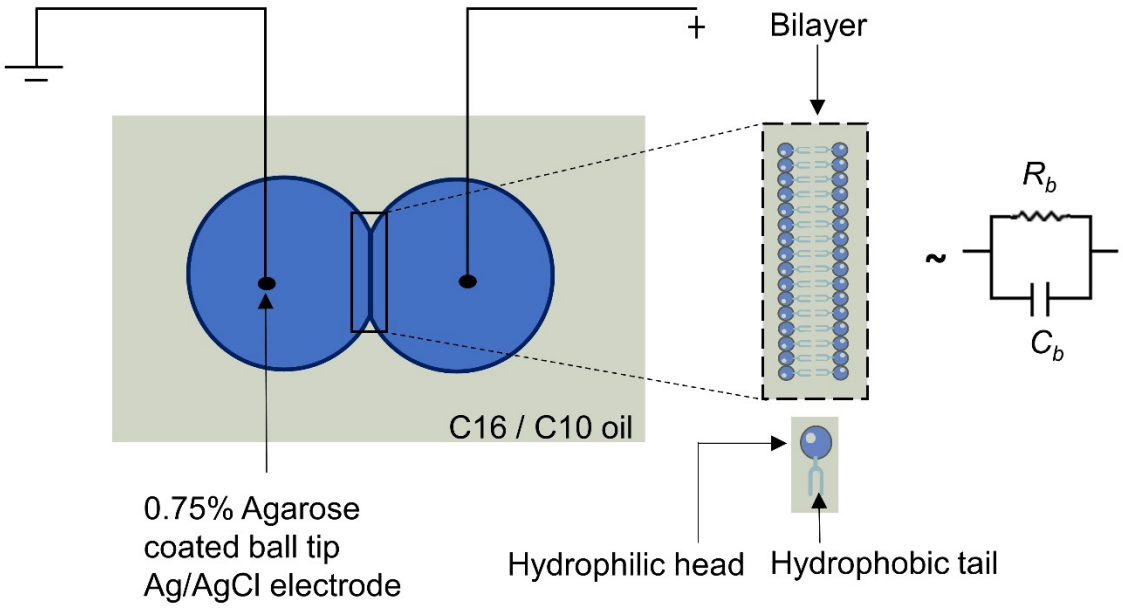

Supplementary Figure S1. Experimental setup used to assemble and characterize droplet-interface bilayer-based artificial electrical synapse. Two lipid-encased aqueous droplets in oil are brought in contact to form a planar lipid bilayer. Ag/AgCl electrodes inserted into the droplets enable application of voltage and measurement of ionic current via a patch clamp amplifier. The ball-shaped electrode tips are coated with hydrophilic agarose gel to aid adhesion to the hanging droplets. A 3-axis micromanipulator supporting each electrode/droplet provides accurate droplet positioning and manipulation for the study. The lipid bilayer devoid of any peptides can be modelled as a parallel resistor-capacitor circuit with typical values of 10 GΩ and 0.63 μF/cm^2, respectively for the nominal resistance and specific capacitance [4].

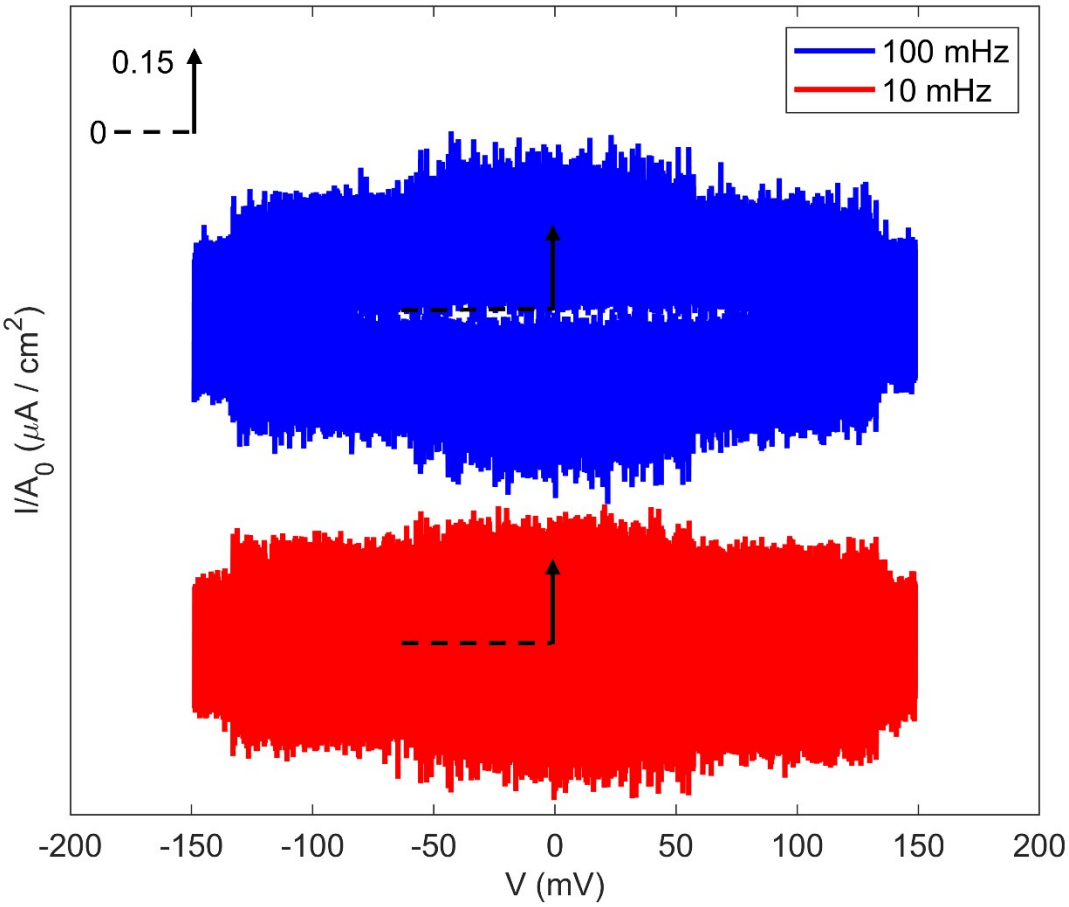

Supplementary Figure S2. *I-V* relationship of an insulating DOPC membrane in hexadecane oil (C16) in response to a 200 mV sinusoidal bias voltage. In absence of any ion conducting gramicidin channels, the elliptical current response stems from frequency-dependent capacitive current.

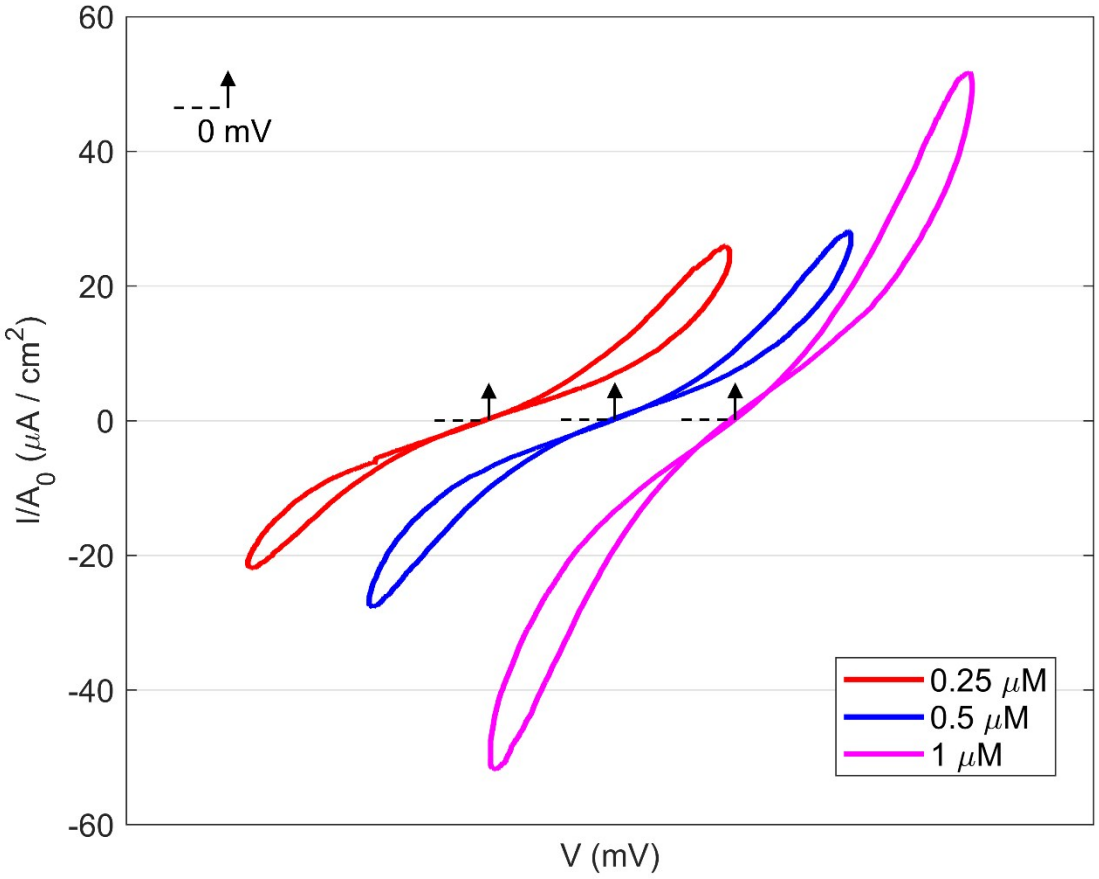

Supplementary Figure S3. *I-V* relationship of AES at varying gramicidin concentrations when excited with 200 mV sinusoidal bias voltage at 10 mHz frequency. The 0 mV pinching points are shifted here for discrete pictorial representation. The data show that increased number of gramicidin pores leads to higher currents due to higher numbers of ions traversing the membrane in the same voltage range.

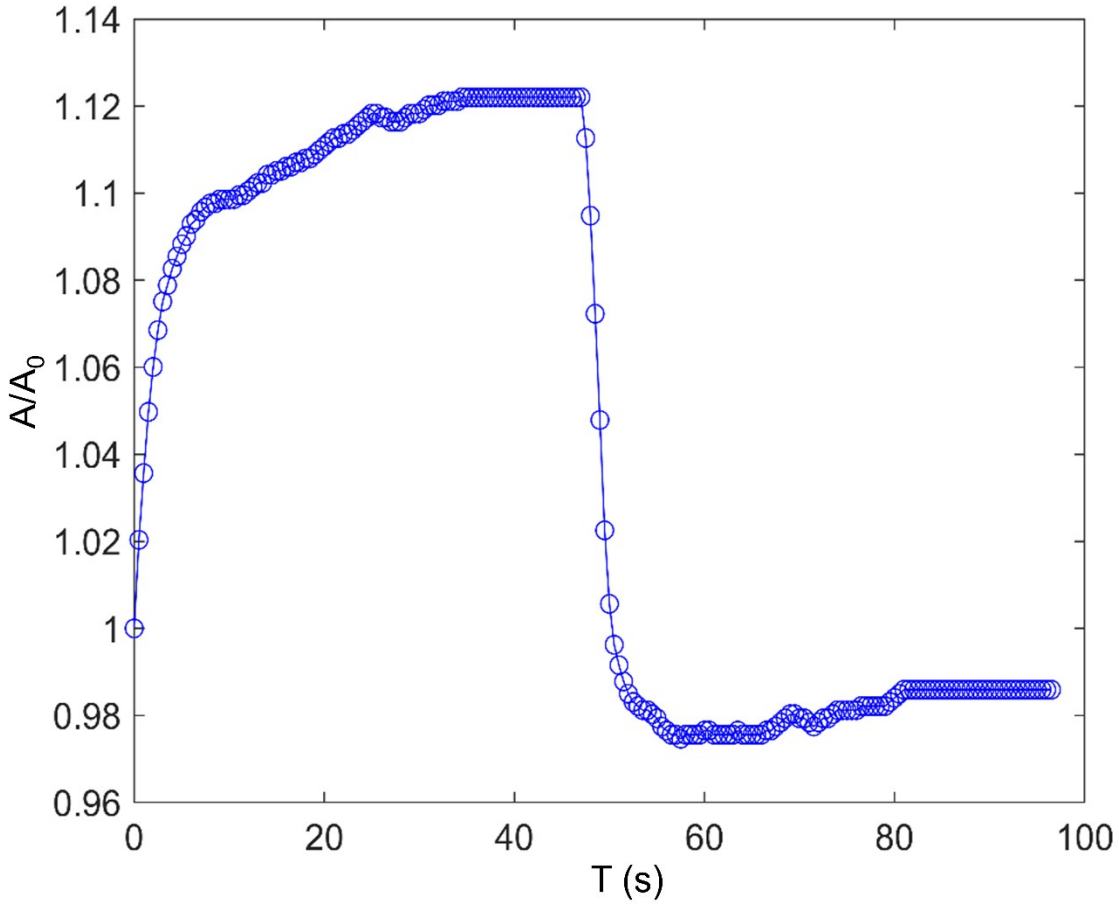

Supplementary Figure S4. Bilayer area growth and decay. The bilayer is allowed to form at 0 mV applied bias. Once the bilayer reaches an equilibrium area, a step voltage of +200 mV is applied for 60 s and then removed. The growth and decay in bilayer area are assessed via image analysis of the connected droplets. For each lipid/oil combination, we report the average time constant from the two dynamic processes.

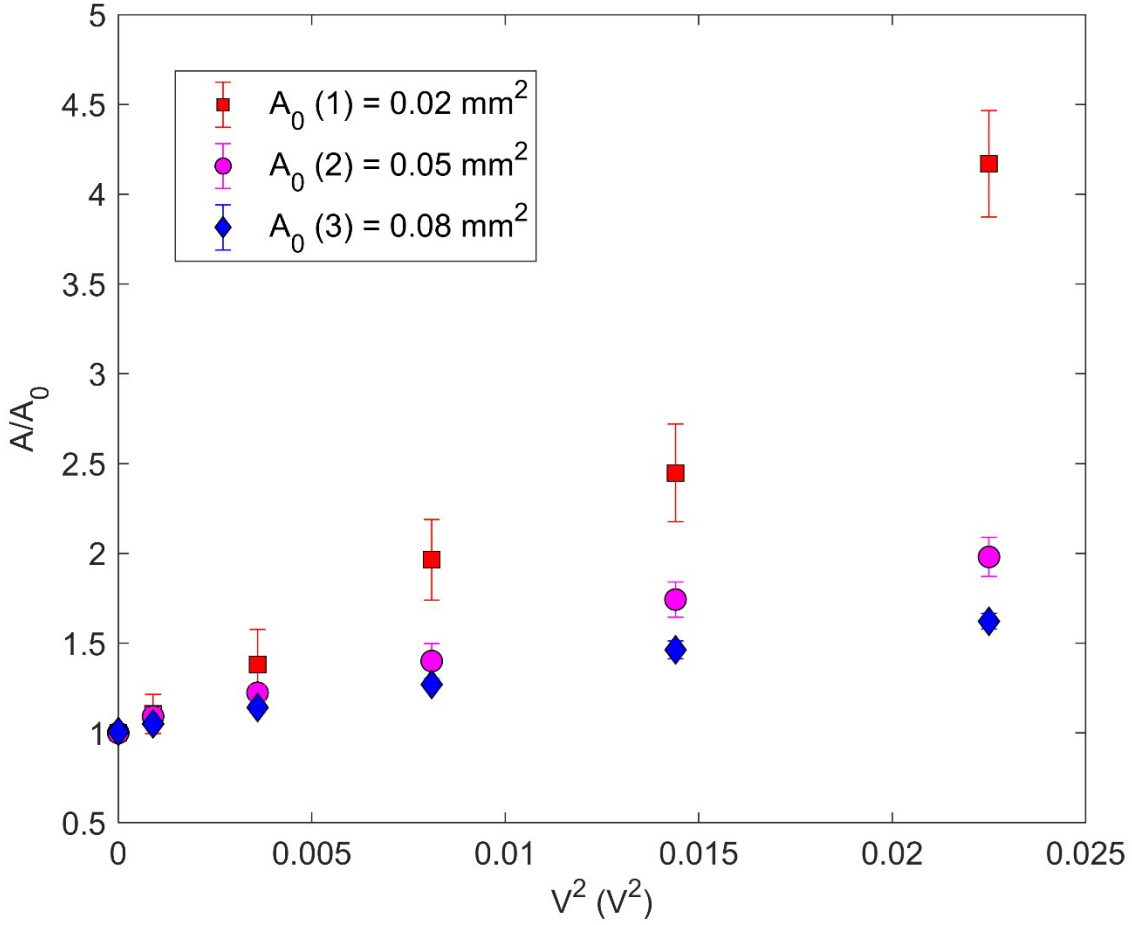

Supplementary Figure S5. Steady-state normalized area of a DOPC bilayer in C16, for different starting areas prescribed through electrode/droplet positioning in response to discrete voltage steps. Each bilayer that forms can have a different nominal area depending on droplet volumes and positioning on electrodes. Therefore, all data reported in the manuscript represent those obtained from bilayers of equal zero-volt areas (either 7.0×10^{-4} cm^2 for C16 or 3.3×10^{-4} cm^2 for C10). To reach this target, the droplets were either brought closer or separated as needed. The data provided here show that when droplets are separated slightly to reduce the nominal area of the bilayer, the membrane exhibits a stronger normalized electrowetting sensitivity.

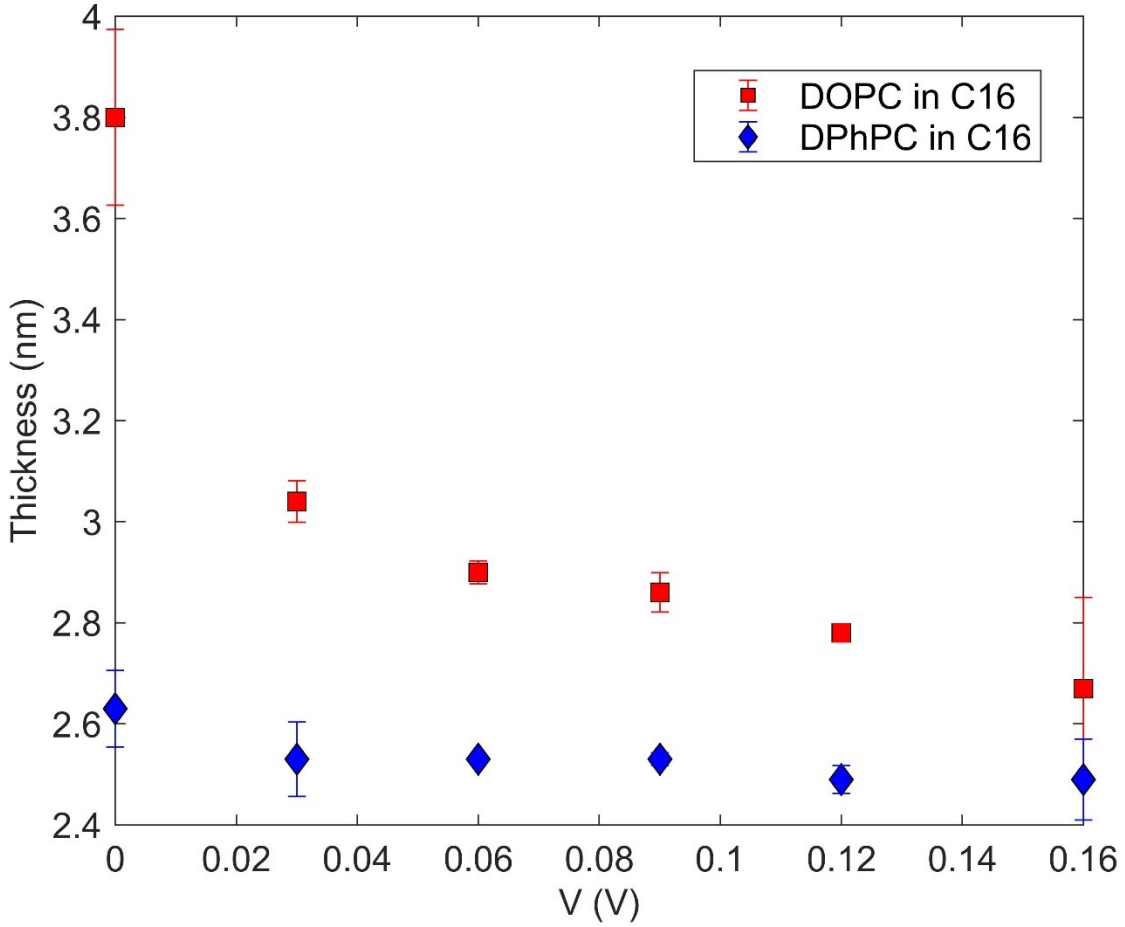

Supplementary Figure S6. Steady-state dielectric thickness versus applied voltage for a DOPC and DPhPC lipid membrane without gramicidin peptides in it. It reflects the thinning of a DOPC from an initially thicker (electrocompression) state in response to increase in bias voltage. Whereas a DPhPC membrane does not undergo significant thinning.

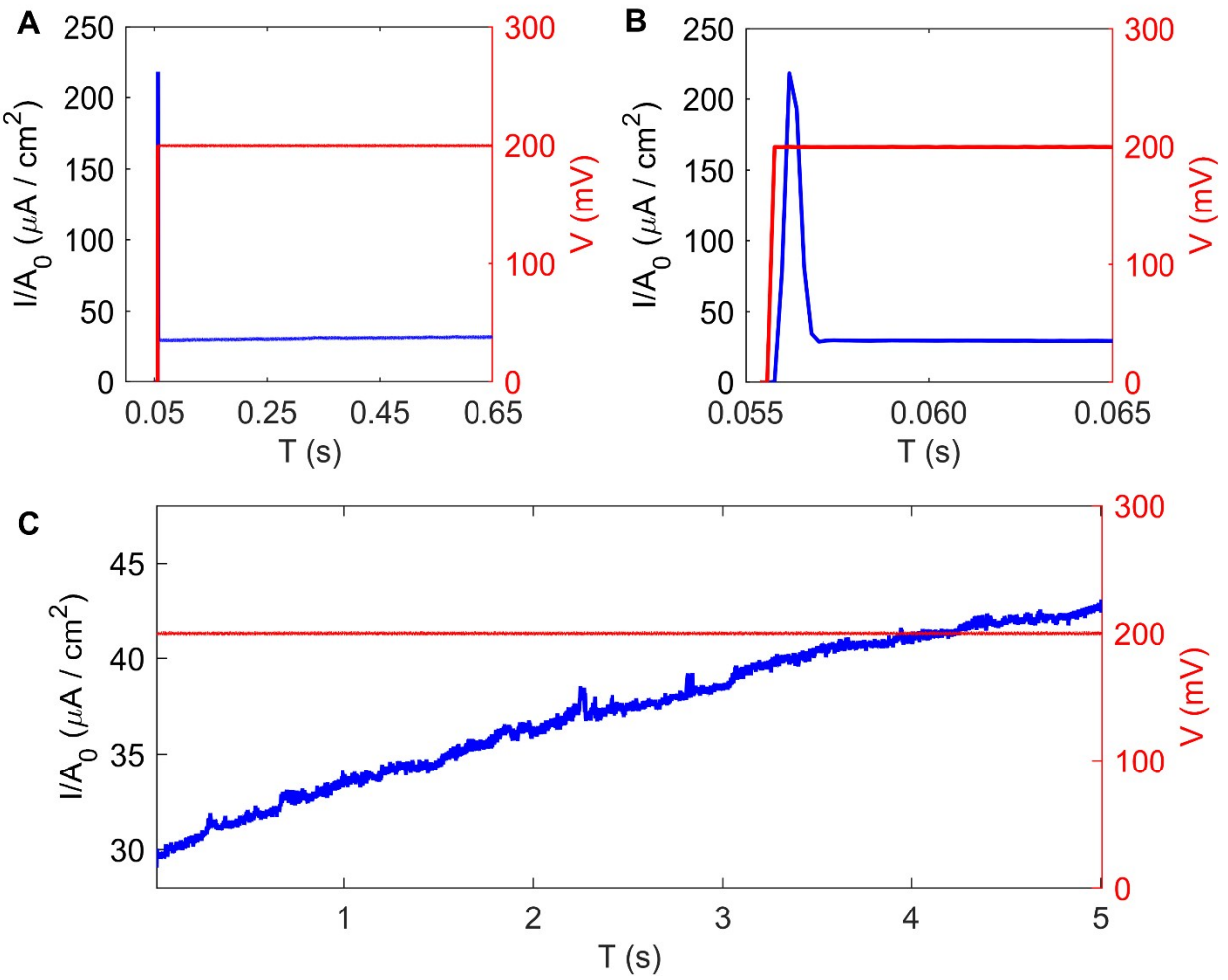

Supplementary Figure S7. Transient current measurements following step-wise changes in applied voltage on a gramicidin-doped DOPC AES formed in C16. (B) is an enlarged representation of (A). The data in (C) show the slower, long-term changes in current that occur at the same time constant of electrowetting, indicating a rise in the number of channels due to an increase in membrane area. Importantly and unlike the work by Bamberg, et al [6, 7] which showed exponential current rises in the first second after a voltage increase, which they used to quantify the kinetics of gramicidin insertion, the data in (A-B) shows that current is flat immediately following the brief capacitive spike. This difference is attributed to much higher concentration of gramicidin used and indicates that the kinetics of channel rearrangement with voltage are nearly instantaneous, which means that hysteretic changes in current are rate-limited by geometrical changes to the bilayer and not due to voltage-dependent channel kinetics.

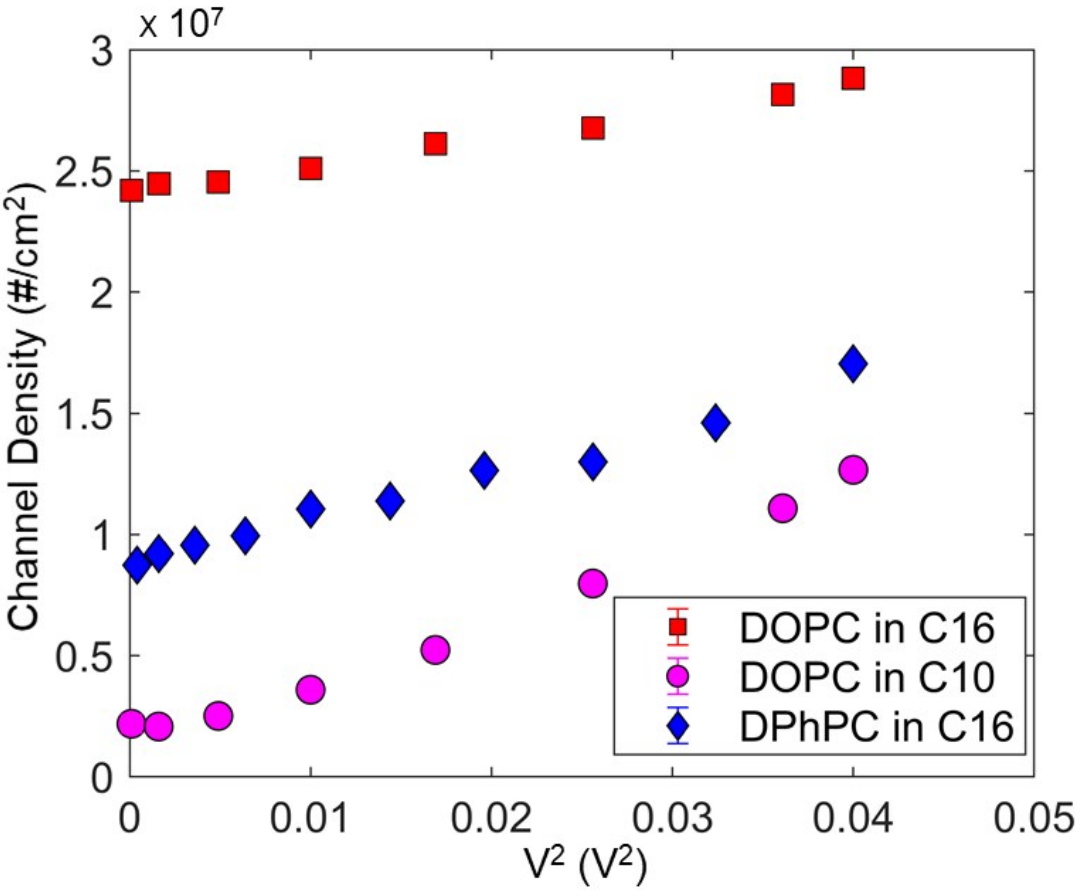

Supplementary Figure S8. Nominal channel density versus voltage for different lipids in both oils (C16 and C10). DOPC in C10 exhibits a lower concentration of channels at 0 mV and a steeper rise with increasing voltage compared to DOPC in C16 or DPhPC in C16. This is due to the fact that DOPC in C10 is thicker at 0 mV (which limits channel insertion) and thins considerably with increasing voltage.

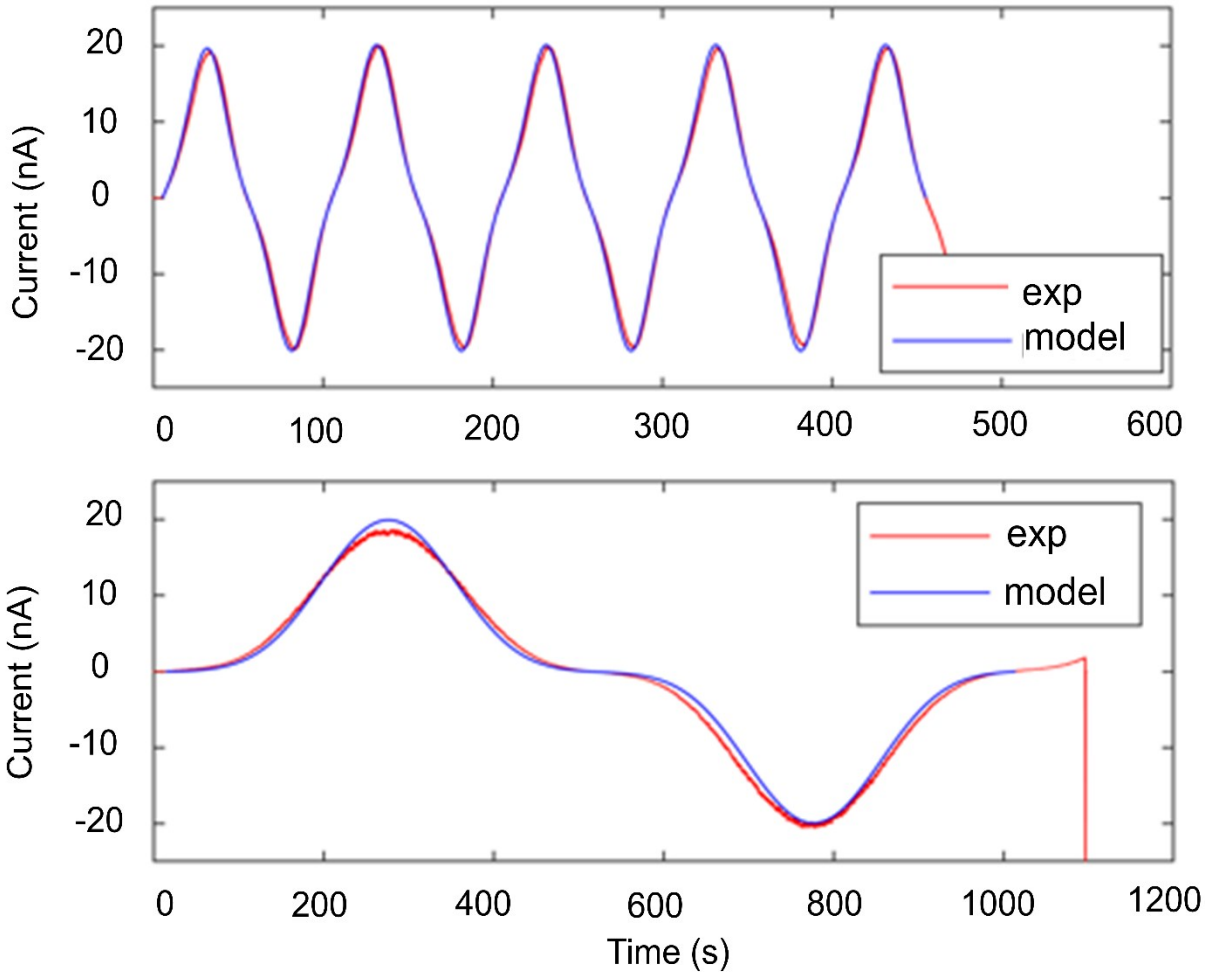

Supplementary Figure S9. Comparison of experimental data (red) and simulated (blue) dynamic current (in blue) for a DPhPC AES in C16 in response to a 0.01Hz, 200mV bias (top) and a DOPC AES in C10 subjected to a 0.001Hz, 200 mV bias (bottom).

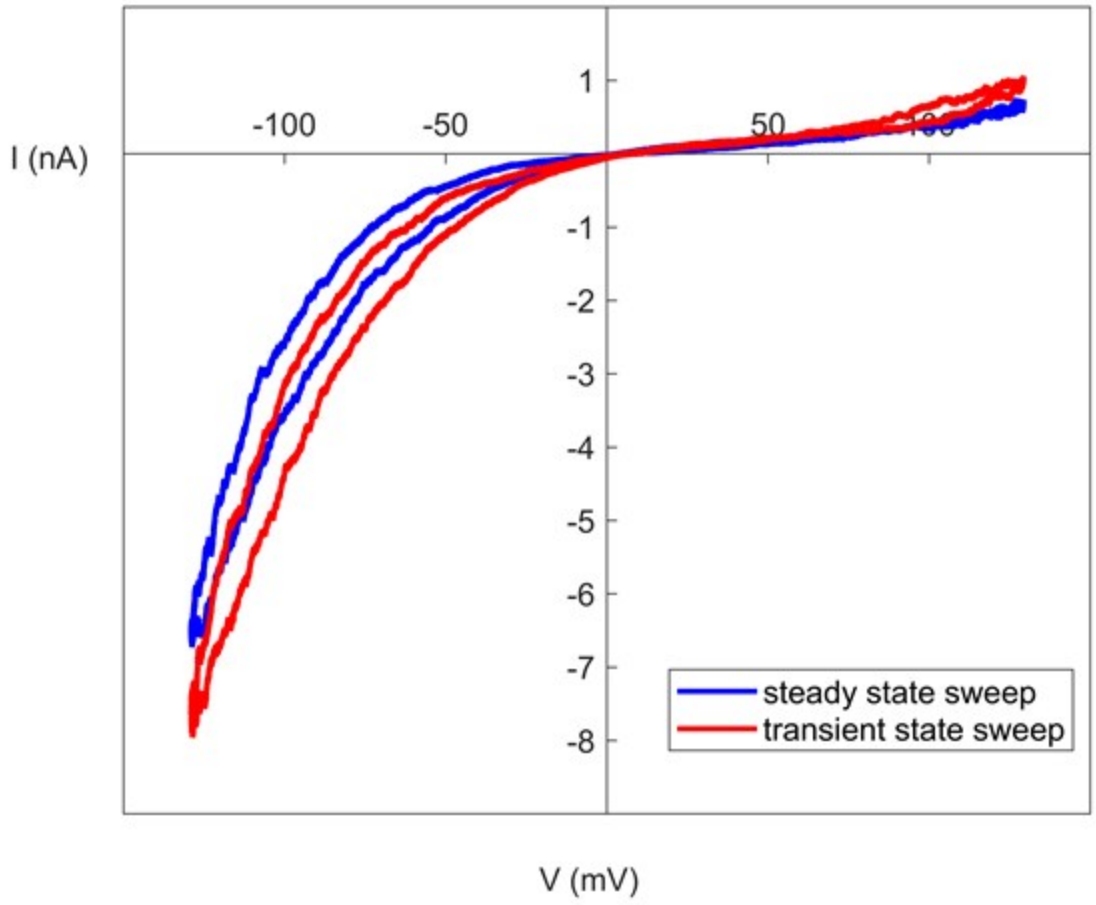

Supplementary Figure S10. *I-V* response of an asymmetric AES consisting of one DOPC leaflet and one leaflet containing a 1:1 molar mixture of DOPC and 1,2-di-O-phytanoyl-sn-glycero-phosphocholine (DOPhPC) and formed in C10 environment to 100 mHz sinusoidal voltage. The red trace depicts the first cycle of the *I-V* sweep, where the device starts from an elevated membrane area (compared to A_0, the area at zero membrane potential) stemming from the non-zero net transmembrane potential difference that exists when 0 mV is applied. The blue trace represents the current response after it has reached steady state conditions of electrowetting (EW) and electrocompression (EC).

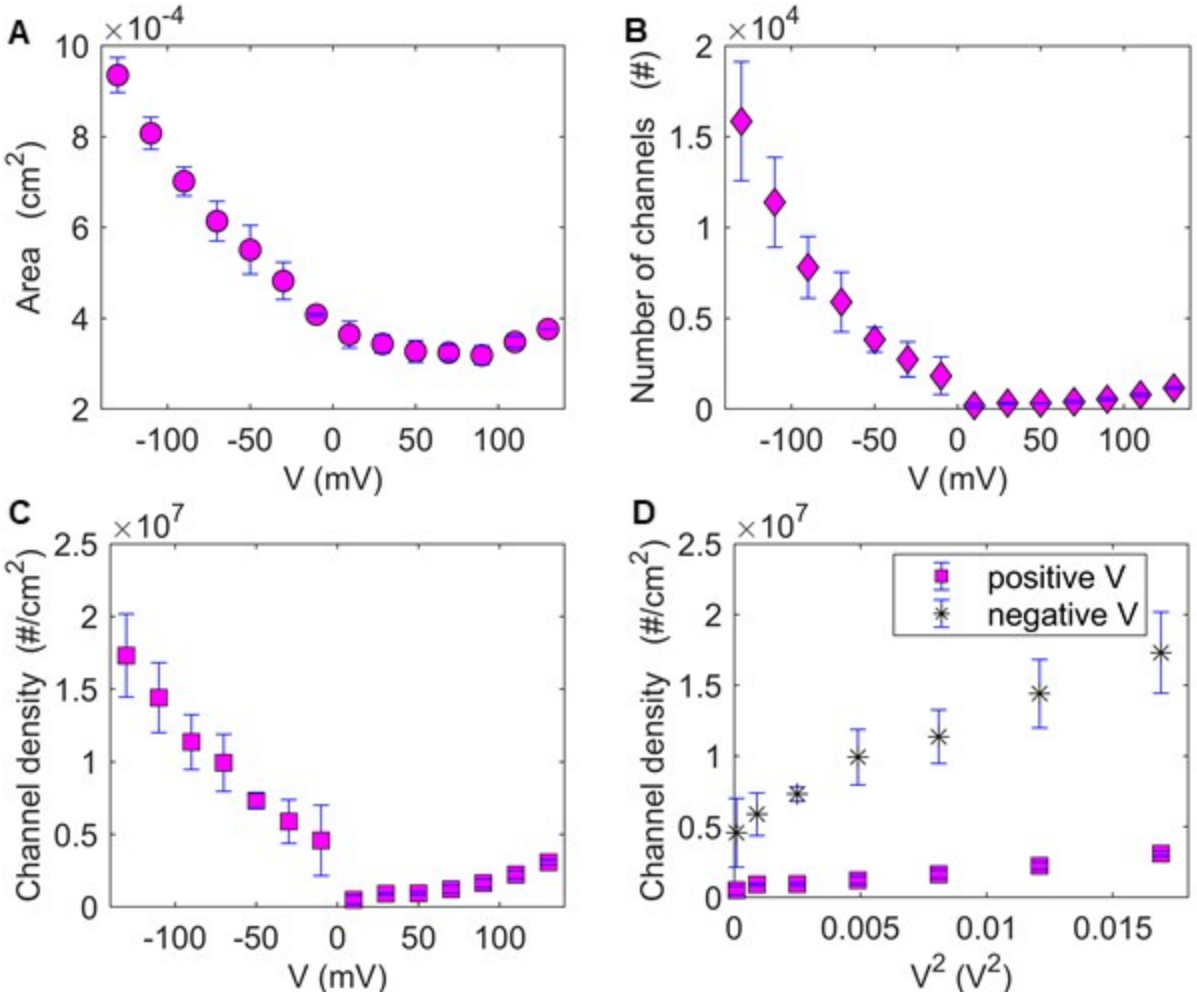

Supplementary Figure S11. Experimental characterization of voltage-dependent state variables for an asymmetric AES. (A) Quasi-static membrane area versus applied voltage reveals a parabolic relationship with a minimum that occurs when the applied voltage is equal and opposite to the intrinsic membrane potential ($v_{int} \approx -85$ mV). The drop in the membrane area with applied positive voltages results from a compensation of net transmembrane potential ($v = v_{appl} + v_{int}$), whereas the steep increase in the area with negative voltages stems from the increase in the total net potential across the membrane. (B) Quasi-static total number of gramicidin channels versus voltage. (C) & (D) displays the rise in channel density which is fueled by an increase in number of channels with voltage and a decrease in membrane area. The slope is steeper for negative voltages because electro compression is playing a crucial role along with electrowetting to help the channels populate the membrane.

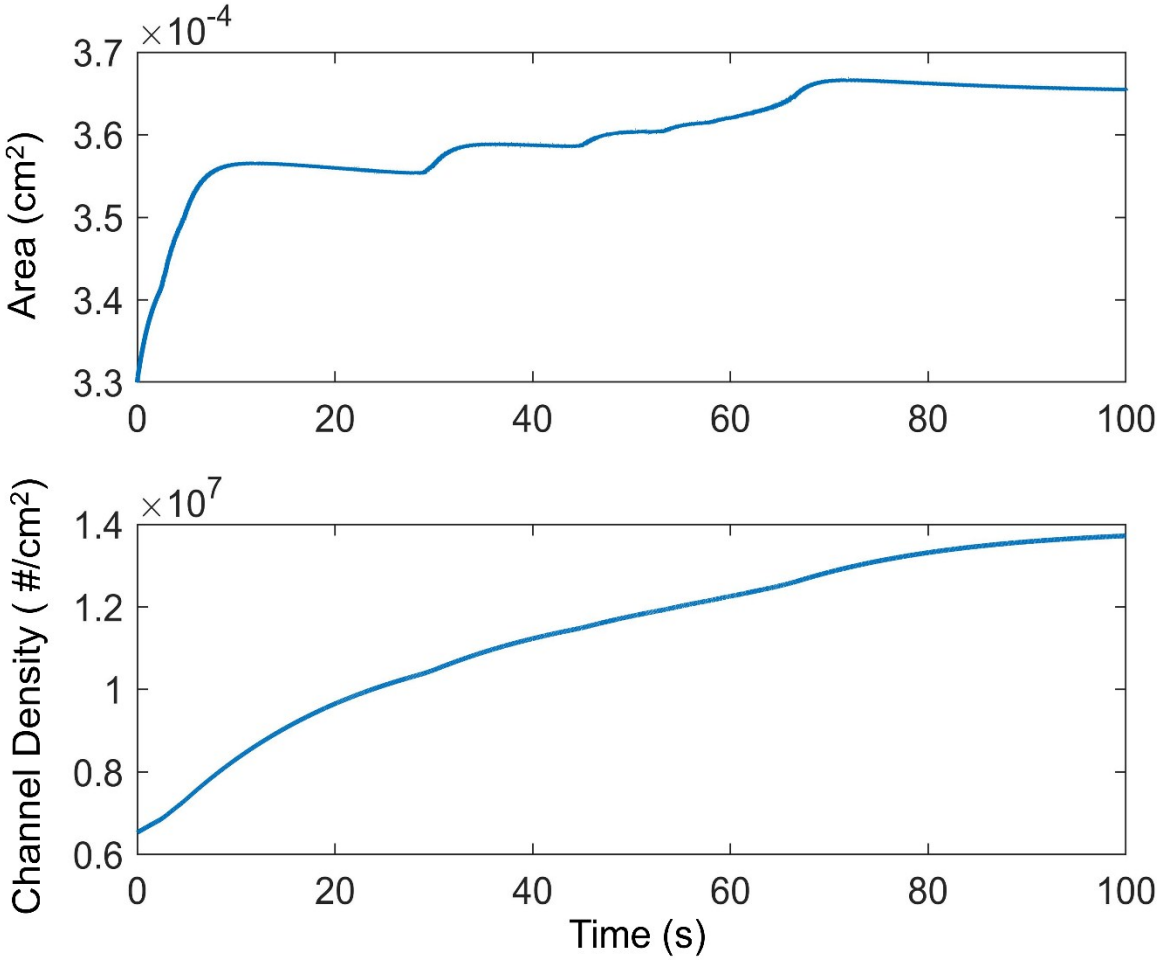

Supplementary Figure S12. Simulated bilayer area (top) and channel density (bottom) versus time for the AES during constant current injection of 10 μA/cm^2 into neuron 1.

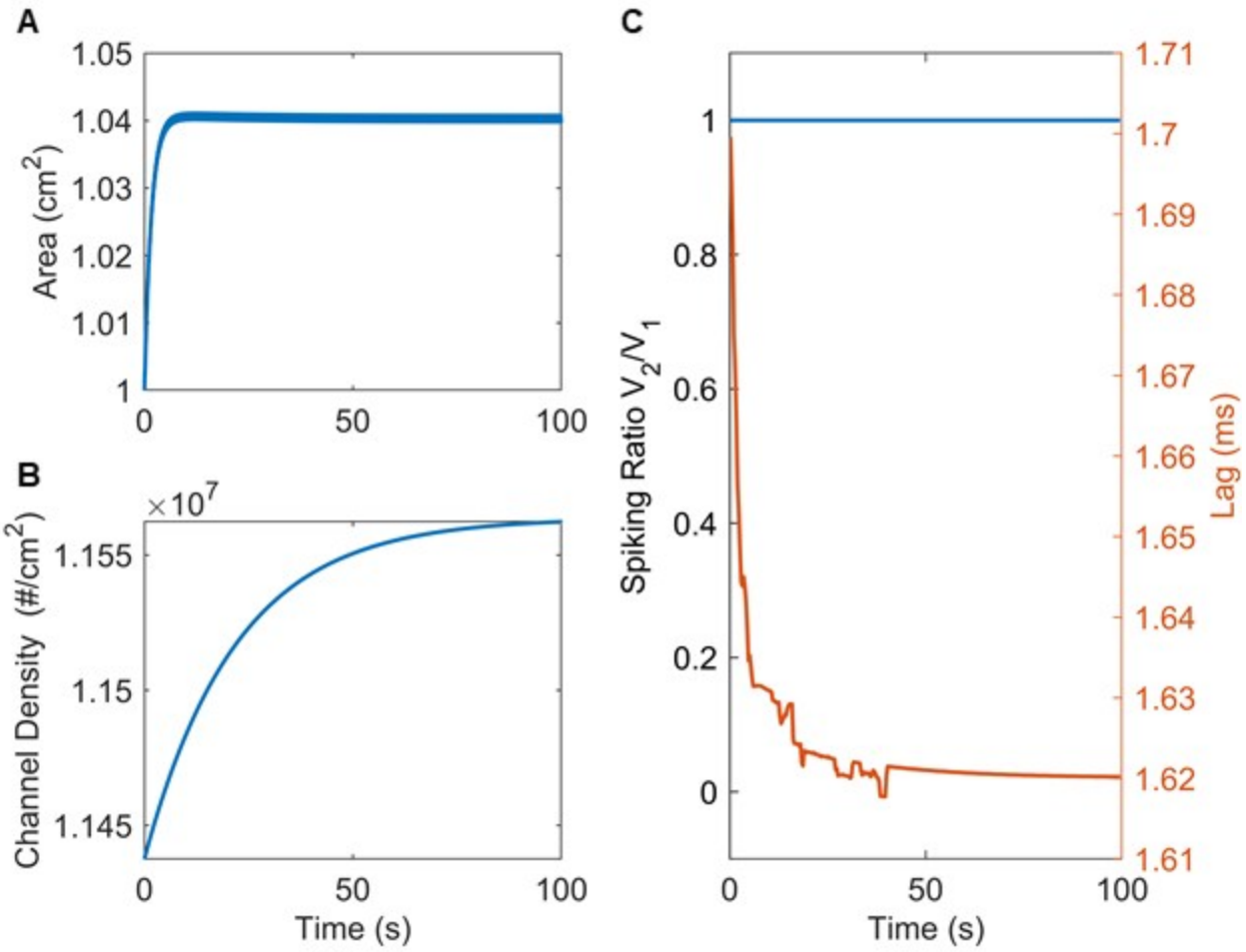

Supplementary Figure S13. Simulation of asymmetric AES interfacing two fully synchronized Hodgkin-Huxley neurons. **(**A, B) Changes in membrane area and channel density versus time (over 100 s). (C) Neuron voltage spiking ratios and lag time versus time. This simulation included a constant current injection of 10 μA/cm^2 into neuron 1 and assumed an initial AES resistance of 30 MΩ, a value low enough to synchronize the action potentials of both neurons. The channel density voltage-dependency was empirically modeled using a linear fit of the quasi-static channel density versus squared voltage data for positive applied potentials (Figure S11D); the fitting results are provided in Supplementary Table S1.

Supplementary Table S1. EW, EC, and gramicidin channel density dependencies on voltage obtained when the membrane area was reduced through mechanical droplet manipulation.

Membrane/Oil	EW area growth		EC thinning	Channel Density $(\times 10^6)$
	τ_{ew} (s)	$\alpha\ (V^{-2})$	τ_{ec} (s)	
DOPC/C10	1.8 ± 0.2 (n=3)	75.3 ± 0.2 (n=4)	22.3 ± 0.3 (n=3)	$N_d(V) = 2000V^2 + 10$
DOPC/C10	1.8 ± 0.2 (n=3)	75.3 ± 0.2 (n=4)	22.3 ± 0.3 (n=3)	$N_d(V) = 10000V^2 + 40$
DOPC: DOPC+DOPhPC/C10	1.8 ± 0.2 (n=3)	69.9 ± 0.2 (n=4)	22.3 ± 0.3 (n=3)	$N_d(V) = 100V^2 + 4.5$

References

1. D. B. Strukov, G. S. Snider, D. R. Stewart and R. S. Williams, *Nature*, 2008, **453**, 80-83.
2. S. H. White and T. E. Thompson, *Biochimica et Biophysica Acta (BBA) - Biomembranes*, 1973, **323**, 7-22.
3. S. H. White and W. Chang, *Biophys J*, 1981, **36**, 449-453.
4. G. J. Taylor, G. A. Venkatesan, C. P. Collier and S. A. Sarles, *Soft Matter*, 2015, **11**, 7592-7605.
5. J. S. Najem, M. S. Hasan, R. S. Williams, R. J. Weiss, G. S. Rose, G. J. Taylor, S. A. Sarles and C. P. Collier, *Nature Communications*, 2019, **10**, 3239.
6. E. Bamberg and P. Läuger, *The Journal of Membrane Biology*, 1973, **11**, 177-194.
7. L. C. M. Gross, A. J. Heron, S. C. Baca and M. I. Wallace, *Langmuir*, 2011, **27**, 14335-14342.